ACS APPLIED MATERIALS & INTERFACES

Forum Article

www.acsami.org

Improving the Gas Barrier Property of Clay–Polymer Multilayer Thin Films Using Shorter Deposition Times

Fangming Xiang,[†] Ping Tzeng,[‡] Justin S. Sawyer,[†] Oren Regev,[§] and Jaime C. Grunlan*,[†]

[†]Department of Mechanical Engineering and [‡]Department of Chemical Engineering, Texas A&M University, College Station, Texas 77843, United States

[§]Department of Chemical Engineering, Ben-Gurion University of the Negev, Beer-Sheva 8410501, Israel

Supporting Information

ABSTRACT: Relatively fast exposure times (5 s) to aqueous solutions were found to improve the gas barrier of clay–polymer thin films prepared using layer-by-layer (LbL) assembly. Contrary to the common belief about deposition time (i.e., the longer the better), oxygen transmission rates (OTRs) of these nano-brick-wall assemblies are improved by reducing exposure time (from 1 min to 5 s). Regardless of composition, LbL films fabricated using shorter deposition time are always thicker in the first few layers, which correspond to greater clay spacing and lower OTR. A quadlayer (QL) assembly consisting of three repeat units of branched polyethylenimine (PEI), poly(acrylic acid) (PAA), PEI and montmorillonite (MMT) clay is only 24 nm thick when deposited with 1 min exposure to each ingredient. Reducing the exposure time of polyelectrolytes to 5 s not only increases this film thickness to 55 nm but also reduces the oxygen transmission rate (OTR) to 0.05 $cm^3/(m^2$ day atm), which is 2 orders of magnitude lower than the same film made using 1 min exposures. A conceptual model is proposed to explain the differences in growth and barrier, which are linked to polyelectrolyte relaxation, desorption, and interdiffusion. The universality of these findings is further exemplified by depositing clays with varying aspect ratios. This ability to quickly deposit high-barrier nanocomposite thin films opens up a tremendous opportunity in terms of commercial-scale processing of LbL assemblies.

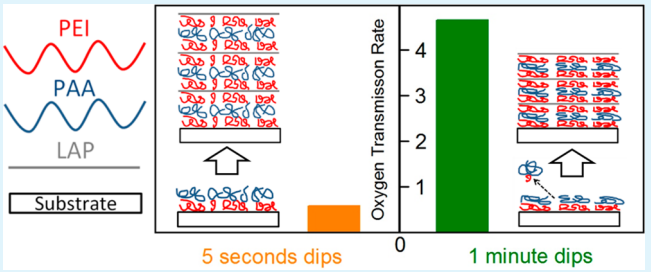

KEYWORDS: *layer-by-layer assembly, deposition time, oxygen barrier, polyelectrolytes, clay*

INTRODUCTION

Clay continues to receive significant attention for its ability to impart mechanical reinforcement,[1−3] gas barrier,[4−6] and even flame retardant characteristics to polymers.[7−10] Conventional clay–polymer composites obtained via melt or solution mixing generally exhibit only modest improvement in their gas barrier property because of insufficient exfoliating and aligning of inorganic nanoplatelets within the organic polymer matrix.[11,12] To prevent aggregation, the clay concentration rarely exceeds 10 wt % in traditional clay–polymer composites.[13−15] Numerous attempts have been made to improve clay exfoliation in polymer matrices, including in situ polymerization and clay functionalization,[16−18] but the improvement in the gas barrier property is still limited by insufficient clay alignment.[19−21] Shear force can be applied to align clay platelets in molten polymer, but Brownian motion of clay platelets (and relaxation of the polymer matrix during solidification) prevents high levels of clay alignment.[13,22,23] A relatively simple method for achieving high clay concentration and alignment is to prepare nanocomposites using the layer-by-layer (LbL) assembly technique.[5,24]

LbL assembly has been widely applied as a simple and versatile thin-film fabrication technique.[25−27] Multifunctional films with controlled structure and composition are prepared by alternating exposure of a substrate to components (usually in water) with complementary interactions. Resultant thin films can exhibit various properties that include gas barrier,[5,28−32] fire retardant,[7,33−35] superhydrophobicity,[36−38] drug delivery,[39−41] and antifogging.[42,43] In the case of clay, a bilayer (BL) film can be constructed by alternately assembling negatively charged platelets with a positively charged polyelectrolyte.[24] Upon deposition of a few BLs, a nano-brick-wall structure with high clay alignment is produced. This structure exhibits remarkable tortuosity for diffusing gas molecules, giving these clay–polymer thin films a super oxygen barrier that rivals SiO_x or metal-oxide-coated films.[44,45]

Improvement in polymer–clay nanobrick walls have been made by switching from BL to quadlayer (QL) recipes, which consist three layers of oppositely charged polyelectrolytes between each clay layer,[28] and also by increasing nanoplatelet aspect ratio.[5,46] For example, it takes 24 BL of branched

Special Issue: Applications of Hierarchical Polymer Materials from Nano to Macro

Received: August 16, 2013
Accepted: November 26, 2013
Published: November 26, 2013

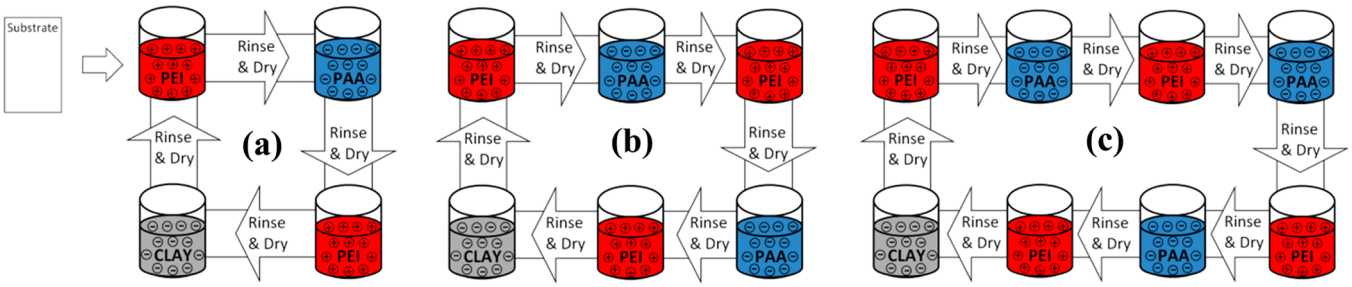

Figure 1. Illustration of the LbL assembly processes for quadlayer (a), hexalayer (b), and octalayer (c) films.

polyethylenimine (PEI) and montmorillonite (MMT) clay (48 individual layers) to achieve an undetectable oxygen transmission rate (OTR < 0.005 $cm^3/(m^2$ day atm)),[47] whereas four PEI/poly(acrylic acid) (PAA)/PEI/MMT QL (16 individual layers) can provide the same level of performance.[28] Further analysis revealed that this improvement in the gas barrier property originated from a more open nano-brick-wall structure. According to a tortuous path model developed by Cussler, instead of following a staircase-like pattern between highly aligned clay layers, gas molecules wiggle laterally while traveling parallel to the diffusion direction (between the clay layers).[48] Greater clay spacing in the QL film provides more room for gas molecule wiggling, leading to a prolonged diffusion length and improved gas barrier property. Despite the success of adding polyelectrolyte layers to transform bilayers to quadlayers, inserting even more polyelectrolyte layers between clay layers may dilute clay concentration and consequently diminish the gas barrier property of these films. With a given clay type, an alternative route to optimize this nano-brick-wall structure involves altering the deposition time used to deposit the polyelectrolyte layers.

A wide range of assertions have been made on the deposition time needed to form a layer (from seconds to hours).[49−52] The general consensus has been the longer the better because the adsorption of polyelectrolyte in each deposition step was typically considered to be an irreversible process involving kinetically frozen cross-links at (or near) the liquid−solid interface.[53−55] Moreover, it was generally accepted that a pronounced change in the adsorbed amount occurs within the first 10 min (or even faster) and a maximum adsorption time of 20 min is needed for saturation (i.e., to reach equilibrium).[56−58] On the basis of these assumptions, typical literature deposition times for LbL assembly are set between 5 and 20 min.[59−61] The present work demonstrates that a shorter dipping time actually leads to thicker clay−polymer films with increased clay spacing and improved gas barrier property. Application of a shorter dipping time during assembly enables clay−polymer LbL films with larger thickness and better gas barrier property to be manufactured using less time and fewer layers. These results suggest that 5 s exposure times are better for LbL films prepared with weak polyelectrolytes and clay platelets. The universality of this discovery may prove to be of great importance as these multifunctional thin films move toward commercialization in a variety of arenas (e.g., protection of electronics, food packaging, and flame-retardant treatments).[34,62,63]

EXPERIMENTAL SECTION

Materials. Laponite (LAP) (Laponite RD) and sodium montmorillonite (MMT) (Cloisite NA^+) clays were purchased from Southern Clay (Gonzales, TX) and used as received. Vermiculite (VMT) (Microlite 963++) clay dispersion was supplied by Specialty Vermiculite Corp. (Cambridge, MA). PEI (M_w = 25 000 g/mol) and PAA (M_w = 100 000 g/mol) were purchased from Sigma-Aldrich (Milwaukee, WI) and used as received. A 1 wt % VMT solution was prepared using 18.2 MΩ deionized water by rolling for 24 h and then allowing for sedimentation of insoluble fractions for another 24 h. All of the other solutions were prepared by simply rolling for 24 h to achieve homogeneity. Prior to deposition, the pH of each PEI solution (0.1 wt % PEI) was altered to 10 using 1 M HCl, and the pH of PAA solutions (0.2 wt % PAA) was altered to 4 using 1 M NaOH. All clay solutions were used at their unaltered pH (1 wt % for VMT, MMT, and LAP).

Substrates. Poly(ethylene terephthalate) (PET) film with a thickness of 179 μm (ST505, DuPont-Teijin) was purchased from Tekra (New Berlin, WI) and used as the substrate for OTR testing and TEM imaging. PET films were rinsed with deionized water and methanol just prior to deposition. Cleaned PET substrates were dried and then treated with a BD-20C corona treater (Electro-Technic Products Inc., Chicago, IL). Corona treatment improves adhesion of the first polyelectrolyte layer by oxidizing the film surface.[64] Single-side-polished silicon wafers were purchased from University Wafer (South Boston, MA) and used to monitor the change in film thickness via ellipsometry. Silicon wafers were cut to 10 × 2 cm strips and then cleaned with piranha solution for 30 min, rinsed with deionized water, acetone, and deionized water again, and dried with filtered air prior to deposition. **Caution:** *These chemicals are dangerous.* Piranha solution reacts violently with organic materials and needs to be handled properly. Polished Ti/Au crystals with a resonance frequency of 5 MHz were purchased from Maxtek (Cypress, CA) and used to monitor mass deposition using a quartz crystal microbalance (QCM).

Layer-by-Layer Deposition. The overall LbL deposition processes for QL, hexalayer (HL), and octalayer (OL) are illustrated in Figure 1. Treated substrates were dipped in the PEI solution for 5 min, rinsed with deionized water, and dried with filtered air. This procedure was followed by an identical dipping, rinsing, and drying procedure in the PAA solution. After this initial bilayer was deposited, different numbers of layers were added to make QL, HL, or OL films under the same rinsing and drying conditions. This procedure was repeated until the desired number of layers was achieved. To study the influence of dipping time on the properties of these films, the dipping time in polyelectrolyte solutions was set at either 5 s or 1 min, whereas the dipping time of clay suspensions remained at 1 min. All thin films were prepared using home-built robotic dipping systems.[64,65]

Film Characterization. Film thickness was measured (on silicon wafers) using an alpha-SE ellipsometer (J.A. Woollam Co., Inc., Lincoln, NE). Films with thickness above 1000 nm or films too hazy for the ellipsometer were measured with a *P*-6 profilometer (KLA-Tencor, Milpitas, CA). Regardless of the measurement method used, the average film thickness was the average of three measurements. The mass of these multilayer films was measured at each quadlayer with a quartz crystal microbalance (QCM) (Inficon, East Syracuse, NY) having a frequency range of 3.8−6 MHz. QCM crystals were cleaned in a PDC-32G plasma cleaner (Harrick Plasma, Ithaca, NY) for 5 min at 10.5 W prior to deposition and were then inserted in a holder and dipped into the corresponding solutions. After each deposition, the crystal was rinsed and dried and then left on the microbalance to

stabilize for 5 min. Oxygen transmission rate measurements were performed by MOCON (Minneapolis, MN) using an Oxtran 2/21 ML oxygen permeability instrument (in accordance with ASTM Standard D-3985) at 23 °C and 0% relative humidity (RH).

Microtomy and TEM Imaging. LbL assemblies were deposited on a PET film, coated with carbon, embedded in Epofix (EMS, Hatfield, PA) resin overnight, and microtomed (Leica Ultracut UCT, Leica, Inc., Germany) to 90 nm thick sections using a Ultra 45° diamond knife (Diatome, Hatfield, PA, 1 mm/s). Thin sections were floated onto water and picked up by 300 mesh copper grids (Ted Pella). The grids were imaged using a Tecnai G2 F20 FE-TEM (FEI, Hillsboro, OR) at an accelerating voltage of 200 kV and analyzed using Digital Micrograph software 3.0.

RESULTS AND DISCUSSION

Influence of Exposure Time on Film Growth and Oxygen Barrier. The influence of exposure time on the growth of all-polymer PEI/PAA bilayer films is shown in Figure 2. Both growth curves have exponential and linear

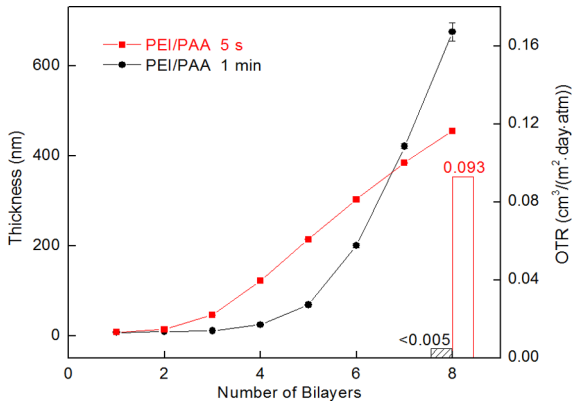

Figure 2. Film thickness as a function of bilayers for PEI/PAA films made with 1 min and 5 s exposure times. The OTR of an eight BL PEI/PAA film with 1 min (from ref 62) and 5 s dipping times is also shown.

growth regions, but there are remarkable differences in thickness. The film prepared using 5 s exposures grows faster in the exponential growth region and exhibits an earlier transition to linear growth (after three BL). In contrast, the film prepared with 1 min dips grows more slowly in the exponential growth zone. It takes five BL to transition to linear growth with this longer exposure time. At the end of exponential growth, both films are thick enough to allow maximum polyelectrolyte interdiffusion, which dominates the linear growth of these films. Consequently, films prepared using 1 min dipping eventually become thicker (at seven BL) than their 5 s counterparts because of the longer interdiffusion time. The thickness of an eight BL film prepared with 1 min dipping (675 nm) is much greater than that made with 5 s dips (455 nm), and this is directly reflected in the gas barrier behavior of these films. As shown in Figure 2, undetectable OTR (<0.005 $cm^3/(m^2$ day atm)) is achieved for an eight BL PEI/PAA film prepared with 1 min dipping,[66] whereas the thinner film made with 5 s dips has an OTR of 0.093 $cm^3/(m^2$ day atm). Although the shorter dipping time appears to require more layers to achieve a high oxygen barrier in all-polymer systems, it can be ideal for clay–polymer assemblies. The addition of clay suppresses polyelectrolyte interdiffusion and thus delays the transition to linear growth, which maintains the films prepared with 5 s dips thicker for more deposited layers.

As can be seen in Figure 3, shorter dipping time yields thicker clay–polymer films for the initial layers deposited, and the addition of clay effectively postpones the overtaking in film thickness. In the case of PEI/PAA/PEI/MMT quadlayers, it takes four QL with 1 min dipping to achieve an undetectable OTR,[28] but the 5 s films remain thicker until nine QL. It is the same situation for $(PEI/PAA)_2$PEI/MMT HL films. It takes three HL prepared with 1 min exposure to achieve undetectable OTR (see the Supporting Information), whereas the overtaking in thickness does not occur until five HL. Because the overtaking in thickness always happens after undetectable OTR is achieved, any 5 s films with measurable OTR are thicker than their 1 min counterparts and should exhibit better gas barrier property. It is interesting to note that the overtaking in thickness also depends on the polymer/clay ratio. The numbers of individual layers needed for overtaking in thickness are 14, 24, 30, and 36 for a BL all-polymer film and OL, HL, and QL clay–polymer films, respectively. As the clay/polymer concentration ratio increases, there will be more clay platelets in the LbL film to block polyelectrolyte interdiffusion, leading to further postponement for the longer dipping time to exceed the shorter thickness.

To illustrate further the thickness overtaking as a result of different exposure time (Figure 3), TEM micrographs of microtomed three and five $(PEI/PAA)_2$PEI/MMT HL films (where the thickness difference is more pronounced) are shown in Figure 4. The clay is easily resolved (dark lines) because of its high electron density in comparison to the polymer (bright regions). Individual clay platelets (1 nm thick, ~100 nm in diameter, white star in Figure 4) are deposited parallel to the substrate in films fabricated with both short and long exposure times. It should be noted that the waviness of the film is probably a result of sectioning. For three HL films, the one prepared with 5 s exposures has a greater overall thickness. The five HL films are quite the opposite, as the sample prepared with 1 min exposures is noticeably thicker. Both results agree well with the ellipsometry measurements in Figure 3b. It is possible to resolves individual clay deposition (Figure 4, top panel) and increased clay-to-clay spacing from the third to the fifth HL, which lines up well with ellipsometric thickness measurements (Figure 3b). The close to perfect matching between the ellipsometry and TEM measurements allows superposition of both in Figure 3b. These TEM images also show that in some cases clay platelets do not fully cover the polymer (Figure 4, black arrow). For films with an equal number of clay layers, a larger overall thickness implies larger clay spacing, which facilitates the perpendicular wiggling of gas molecules with respect to the diffusion direction and consequently increases the diffusion path and gas barrier behavior.[24,28,67,68]

The mass of PEI/PAA/PEI/MMT layers with different dipping times was measured with QCM and is shown in Figure 5. Similar to the trend observed for thickness in Figure 3a, both films have linear and exponential growth regions, with 5 s dipping producing more mass before nine QL. The density of these quadlayer films was calculated by dividing the mass by the film thickness and the area of the film deposited on the crystal. It should be noted that small errors in film mass and thickness can be compounded to produce a much greater scattering in density. Moreover, the density of films prepared with 1 min dipping shows more variation because of the longer interdiffusion time, which could magnify the film thickness deviation and ultimately lead to larger density variation. As can

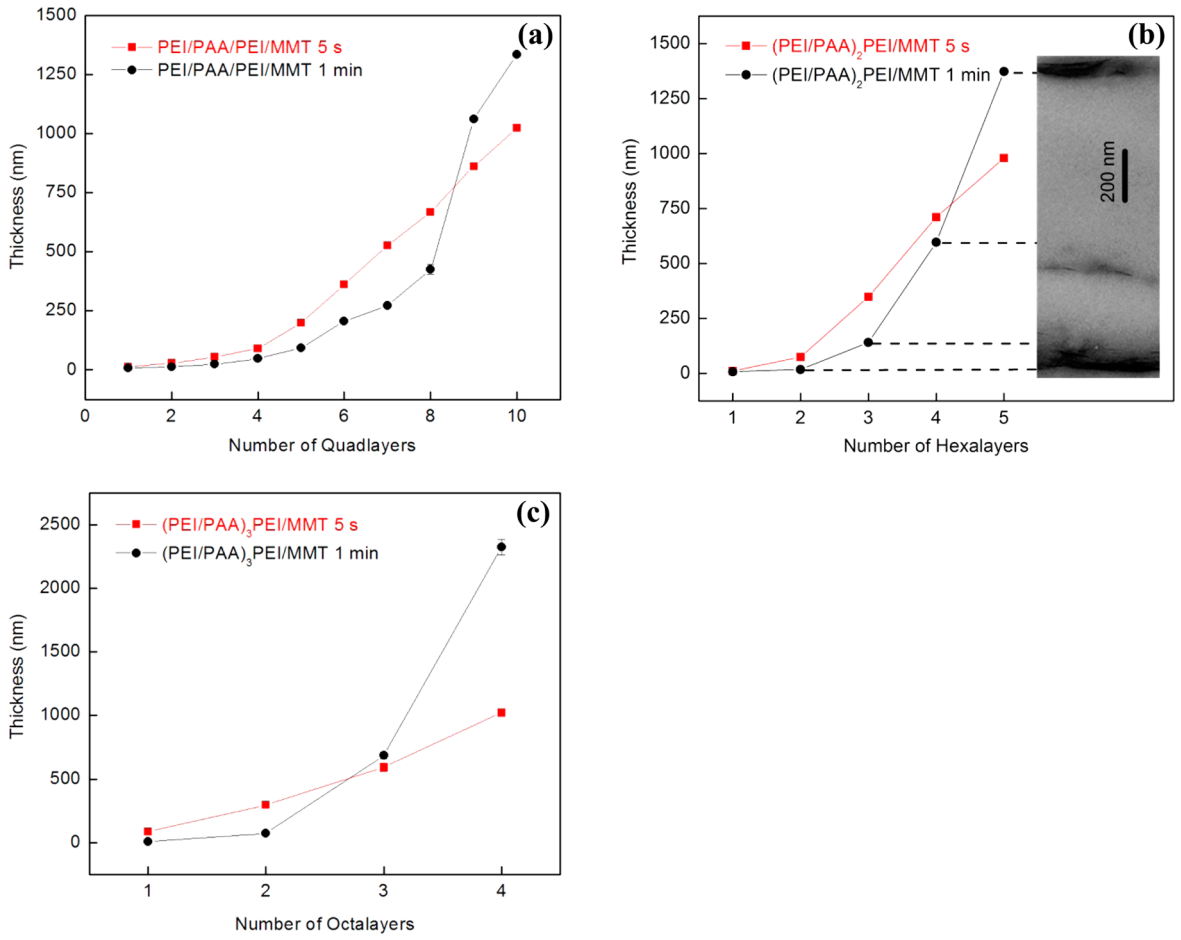

Figure 3. Film thickness as a function of quadlayers (a), hexalayers (b), and octalayers (c) deposited using 5 s and 1 min dipping times. The growth curve of hexalayer films, prepared using 1 min dipping, is correlated to the TEM micrograph of a five HL film in panel b.

be seen in Figure 5b, the short dipping time creates films with a lower initial density, but it increases with an increasing number of quadlayers (up to four QL). The opposite is true for the film with 1 min dipping times, which has a higher density initially but decreases with an increasing number of quadlayers (and then oscillates around 1.25 g/cm^3 after four QL). Although dipping time results in different initial densities, this difference gradually disappears as the number of quadlayers deposited increases.

Influence of Clay Size on Film Growth. To confirm further the role of clay in this process, QL films with different types of clay were prepared. Each clay type has a thickness of about 1 nm, and the average diameters of LAP, MMT, and VMT are 25, 200, and 1100 nm, respectively.[5,8] As shown in Figure 6, the overtaking in film thickness happens the earliest in the PEI/PAA/PEI/LAP film (at seven QL). After switching to the larger diameter MMT, the overtaking in film thickness is postponed to nine QL (Figure 3a). VMT-based films further extend the number of layers needed for the longer dip time to overtake 5 s dips in thickness (at 10 QL). Detailed growth curves for LAP and VMT quadlayers can be found in Figure S1 (Supporting Information). VMT has the largest diameter and is therefore the most effective in suppressing polyelectrolyte interdiffusion. These results suggest that the extent of thickness postponement can be tailored by changing the clay/polymer concentration ratio and/or clay aspect ratio. It is also known that clay aspect ratio influences barrier properties of these thin films, with a greater diameter producing a lower transmission rate for a given number of layers.

The influence of dipping time on the thickness, oxygen transmission rate, and permeability of three QL films prepared with three different clays is shown in Figure 7 and Table 1. It is interesting to note that regardless of the clay type, a short dip time always leads to a lower OTR, which is directly linked to film thickness. As can be seen in Figures 3a and 6, a shorter deposition time always generates a thicker film for at least the first seven QL. All films used for OTR testing were three quadlayers, so those made with 5 s exposures are thicker than those prepared with 1 min. With all of the films having the same number of clay layers, a larger film thickness means a larger average clay spacing and an elongated diffusion path for gas. In addition to the exposure time, the diameter of the clay also plays an important role on the OTR of these thin films. As can be seen for the films prepared with 5 s dips, larger diameter clays generate films with a better oxygen barrier (Figure 7). VMT has the largest average diameter and the lowest OTR in films prepared with 5 s exposures, but this is not the case for VMT-based films prepared using 1 min dipping. This unexpected increase in OTR may originate from the desorption of polyelectrolytes. The desorption of low-molecular-weight polyelectrolytes from the film surface could create voids and reduce the number of available bonding sites (discussed in more detail in the next section). These surface defects may not cause a problem for the subsequent deposition of polyelec-

dx.doi.org/10.1021/am403445z | ACS Appl. Mater. Interfaces 2014, 6, 6040−6048

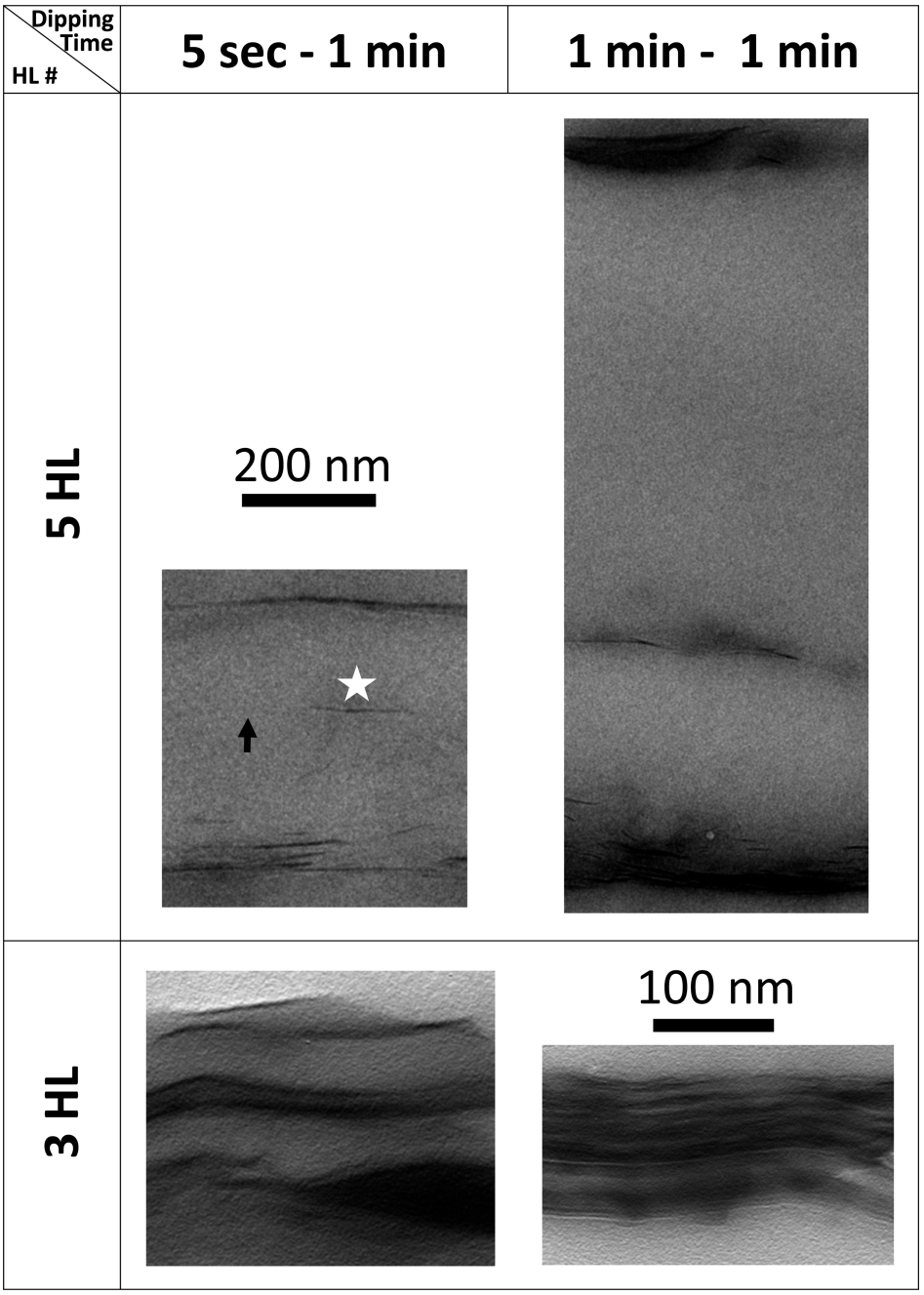

Figure 4. TEM cross-sectional images of three and five hexalayer films deposited using 5 s and 1 min polyelectrolyte exposure times. Arrow, partial clay coverage; star, individual clay platelet (~100 nm in diameter). The growth direction is from bottom to top.

trolytes because of the relatively coiled conformation and inherent flexibility of the polyelectrolyte chains, but they may diminish the adsorption of clay. It is likely that the larger the clay platelets, the higher the negative impact on adsorption. Successful adsorption of larger clay platelets may require the establishment of many bonds with the underlying surface, leading to the largest negative impact on VMT.

Growth Mechanism for Clay–Polymer Assemblies. It has been shown that a shorter exposure time deposits a thicker (Figure 3) and heavier (Figure 5a) film in the first few layers. This result seems counterintuitive because it has been generally accepted that the adsorption of polyelectrolyte at each deposition step is kinetically irreversible.[53−55] Several studies have suggested that the adsorption process requires 10−20 min to reach saturation.[50,57,58,69] On the basis of the aforementioned assumptions, typical dipping times continue to be set between 5 and 20 min.[70−73] Although these assumptions work well for strong polyelectrolyte assemblies, they are unreliable for weak polyelectrolytes. Unlike with strong polyelectrolytes, the linkage between two weak polyelectrolytes (or weak−strong polyelectrolytes combinations) cannot be considered frozen. It has been demonstrated that it is possible for polyelectrolytes that were already integrated into a multilayer assembly to be exchanged by polyelectrolytes in solution, breaking and reforming ionic cross-links between them in the process.[53,74,75] The active nature of these linkages is also exemplified in the desorption of polyelectrolyte from these assemblies.[76−78] When weak polyelectrolyte chains are

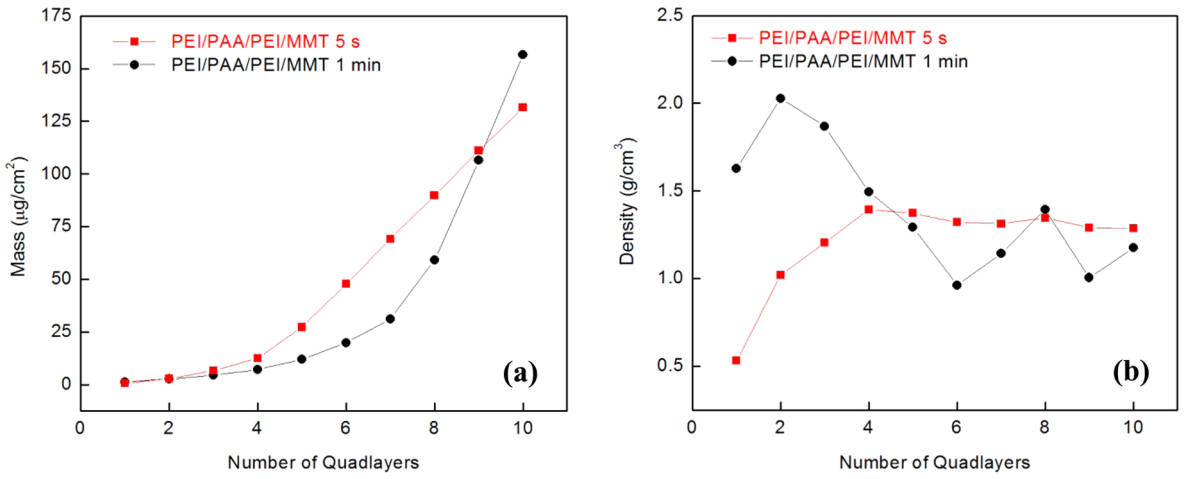

Figure 5. Mass (a) and density (b) of films prepared using different dipping times as a function of quadlayers deposited.

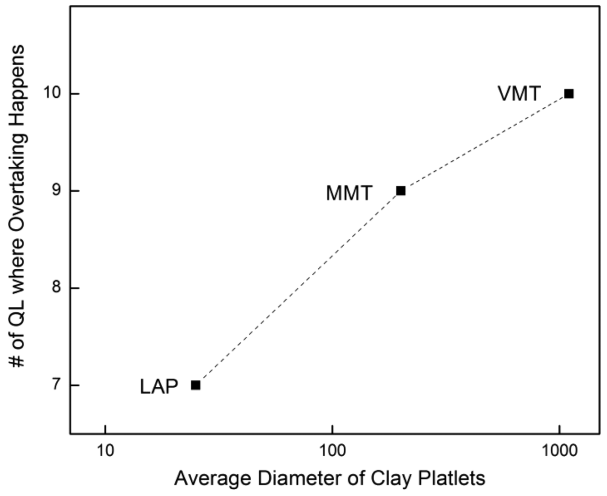

Figure 6. Number of quadlayers where overtaking occurs as a function of the clay diameter.

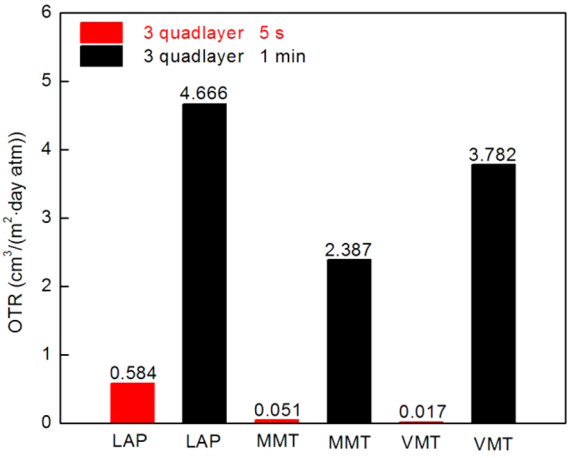

Figure 7. Oxygen transmission rate of three quadlayer films fabricated with LAP, MMT, and VMT using 5 s and 1 min dipping times.

adsorbed onto an oppositely charged substrate, the individual chains are only weakly bound. Increasing the exposure time of this step only induces more relaxation of the polymer chains.[79] The difference between the long and short dipping times will not show up until another layer of oppositely charged polyelectrolyte is added. Incoming polyelectrolyte chains will initially adhere to the surface and then form either soluble complexes in solution or a multilayer on the surface. If the enthalpic gain from electrostatic interactions is small, then the formation of soluble complexes in solution will be more favorable on the basis of entropic considerations.[80,81] In this case, the best way to minimize desorption is to reduce deposition time. It has already been shown that thicker all-polymer LbL assemblies can be produced if a shorter dipping time is used to minimize the desorption of polyelectrolytes.[77,78]

Summarizing the analysis, the hypothesized growth mechanism of these clay−polymer multilayers in the first three QL is illustrated in Figure 8. The film prepared with a 5 s dip time will be thicker and heavier because there is not enough time for the polyelectrolytes to relax into a more extended conformation or to desorb from the surface. In contrast, films prepared with 1 min deposition steps are thinner and lighter. There is no desorption of polycations in the first layer, but the film prepared with a longer deposition time is slightly thinner because of the longer time required for the polycation chain to relax. Upon dipping into the oppositely charged solution, lower molecular weight polycations are more likely to desorb from the surface by interacting with polyanions in solution and forming soluble complexes.[78] In the meantime, polyanions already adsorbed on the surface will continue to relax and adopt a more flattened conformation, leading to an even thinner film. The addition of a third polycation layer will be similar to that of the second layer in terms of the desorption and relaxation of polyelectrolytes. The addition of a fourth clay layer completes one full quadlayer. With each quadlayer made using 1 min dips being thinner than that using 5 s dips, the overall thickness of a three QL film will be thinner with the longer deposition time.

It should be noted that the proposed mechanism illustrated in Figure 8 describes only the growth of these assemblies in the first few quadlayers, where the influence of polyelectrolyte interdiffusion is not dominant. As these clay-based multilayers get thicker, they will transition to linear growth, where polyelectrolyte interdiffusion will be fully realized and become the predominant force. In the linear growing region, the effect of polyelectrolyte relaxation is negligible because the interdiffusion-driven deposition leads to a much greater film thickness and mass.[66,82,83] In this regime, polyelectrolyte interdiffusion also eliminates the desorption of polyelectrolytes from the assembly.[78] Consequently, every QL fabricated using

dx.doi.org/10.1021/am403445z | ACS Appl. Mater. Interfaces 2014, 6, 6040−6048

Table 1. Properties of Three Quadlayer Films Fabricated with Various Diameter Clays and Exposure Times

3 QL film recipe	film thickness (nm)	OTR ($cm^3/(m^2$ day atm))	permeability ($\times 10^{-16}$ cm^3 cm/(cm^2 s Pa))	
			film[a]	total
PEI/PAA/PEI/LAP 5 s	58.08	0.584	0.00083	1.19
PEI/PAA/PEI/MMT 5 s	55.09	0.051	0.000064	0.10
PEI/PAA/PEI/VMT 5 s	85.06	0.017	0.000033	0.034
PEI/PAA/PEI/LAP 1 min	22.24	4.666	0.0052	9.54
PEI/PAA/PEI/MMT 1 min	24.12	2.387	0.0018	4.88
PEI/PAA/PEI/VMT 1 min	30.71	3.782	0.0047	7.74

[a]Film permeability was decoupled from the total permeability using a previously described method.

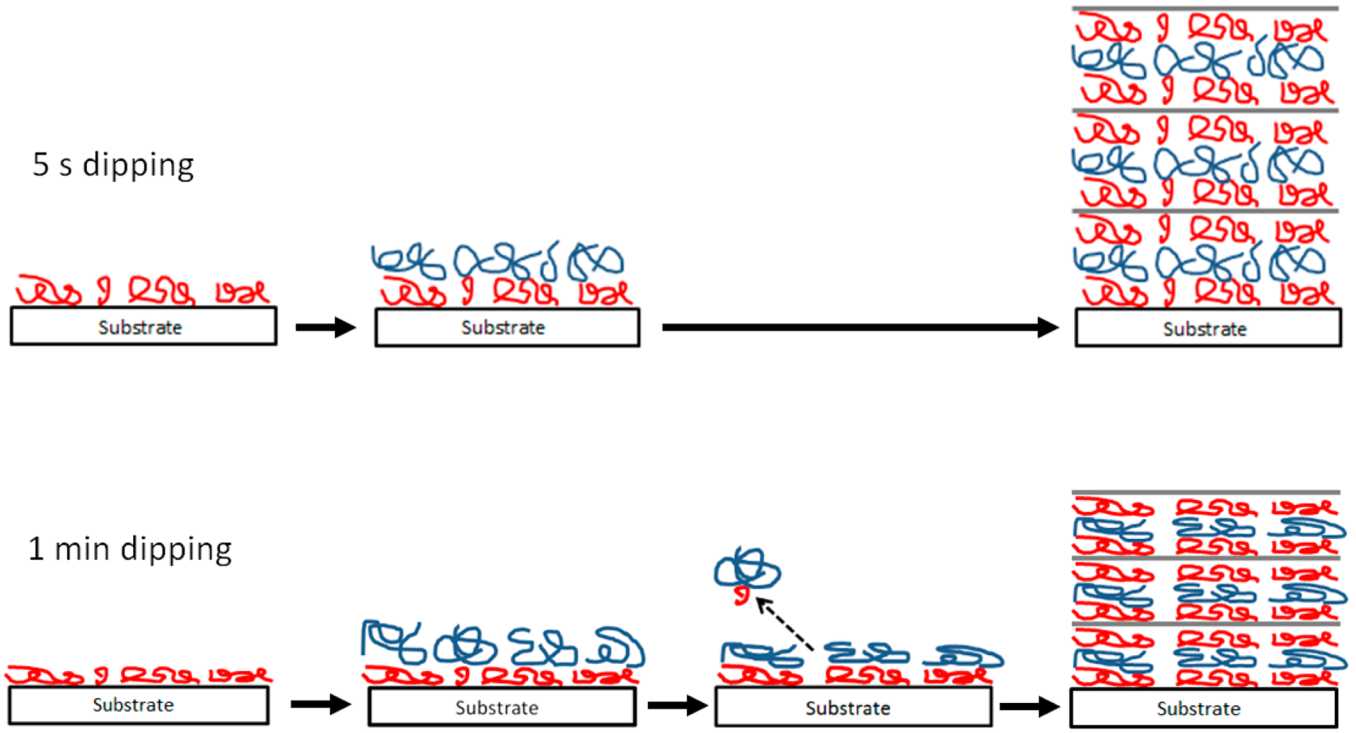

Figure 8. Illustration of the layer-by-layer deposition process for three quadlayer films fabricated using 5 s and 1 min deposition times. The red, blue, and gray lines represent polycation, polyanion, and clay, respectively.

1 min deposition is thicker than that made with 5 s exposures in the linear growth region, ultimately causing the overtaking in film thickness. This relationship between polyelectrolyte interdiffusion and film thickness also explains why the overtaking can be postponed or expedited by altering the clay/polymer concentration ratio and clay diameter, as shown in Figures 3 and 6. This proposed growth mechanism also agrees with the observed changes in thin-film density (Figure 5b). In the first few quadlayers, the film prepared with 1 min dipping is more densely packed because of the relaxation of polyelectrolytes chains. As more layers are deposited and the polyelectrolyte interdiffusion develops, it begins to dominate the change in film thickness and the packing of the multilayer assembly, eventually eliminating the difference in the density beyond four QL.

CONCLUSIONS

LbL polyelectrolyte deposition time was found to have a significant influence on the growth and gas barrier property of clay–polymer assemblies. Regardless of the thin-film composition, a shorter dipping time always produced a thicker film in the first few layers. This unique behavior is due to the differing growth mechanisms in the exponential and linear growing regions. During exponential growth, polyelectrolyte interdiffusion is not fully developed, and the growth of the multilayer film is controlled by desorption and relaxation of oppositely charged polyelectrolytes. Films prepared with 5 s dip times are thicker and heavier because there is little time for desorption and relaxation. Linear growth, however, is primarily controlled by polyelectrolyte interdiffusion, which allows films prepared with 1 min dips to be eventually thicker and heavier. Shorter dipping time turns out to be ideal for clay–polymer assemblies because the addition of clay suppresses polyelectrolyte interdiffusion and effectively postpones the thickening achieved with longer dips. These results are supported by cross-sectional images and ellipsometric thickness measurements. Altering the clay/polymer concentration ratio and clay diameter provides a way to tailor further the growth and barrier characteristics of multilayer thin films by controlling the extent of polyelectrolyte interdiffusion. The OTR of a film prepared with 5 s dips decreases with increasing clay diameter, and films prepared with this short exposure time always have a lower OTR than their 1 min counterparts. The short dipping time may even help to reduce the number of layers needed for certain applications,

which would reduce processing cost and time. For instance, the MMT-based quadlayer used to require four QL with 1 min dipping to achieve an OTR lower than 0.5 $cm^3/(m^2$ day atm).[28] In contrast, this level of oxygen barrier requires only three QL with 5 s dips. This finding is very important because it demonstrates the ability to make useful thin films very quickly, improving the outlook for industrial-scale development of the LbL assembly technique.

■ ASSOCIATED CONTENT

Supporting Information

Properties of three hexalayer films fabricated with MMT using different dip times. Detailed film thickness as a function of quadlayers deposited with LAP and VMT. This material is available free of charge via the Internet at http://pubs.acs.org.

■ AUTHOR INFORMATION

Corresponding Author

*Tel.: +1 979 845 3027; Fax: +1 979 862 3989; E-mail: jgrunlan@tamu.edu.

Notes

The authors declare no competing financial interest.

■ ACKNOWLEDGMENTS

We thank the Texas A&M Engineering Experiment Station (TEES), Kuraray, and The Dow Chemical Company for financial support of this research.

■ REFERENCES

(1) Pavlidou, S.; Papaspyrides, C. D. *Prog. Polym. Sci.* **2008**, *33*, 1119−1198.
(2) Ojijo, V.; Sinha Ray, S.; Sadiku, R. *ACS Appl. Mater. Interfaces* **2012**, *4*, 2395−2405.
(3) Phua, S. L.; Yang, L.; Toh, C. L.; Huang, S.; Tsakadze, Z.; Lau, S. K.; Mai, Y.-W.; Lu, X. *ACS Appl. Mater. Interfaces* **2012**, *4*, 4571−4578.
(4) Choudalakis, G.; Gotsis, A. D. *Eur. Polym. J.* **2009**, *45*, 967−984.
(5) Priolo, M. A.; Holder, K. M.; Greenlee, S. M.; Grunlan, J. C. *ACS Appl. Mater. Interfaces* **2012**, *4*, 5529−5533.
(6) Najafi, N.; Heuzey, M. C.; Carreau, P. J. *Compos. Sci. Technol.* **2012**, *72*, 608−615.
(7) Laufer, G.; Kirkland, C.; Cain, A. A.; Grunlan, J. C. *ACS Appl. Mater. Interfaces* **2012**, *4*, 1643−1649.
(8) Kiliaris, P.; Papaspyrides, C. D. *Prog. Polym. Sci.* **2010**, *35*, 902−958.
(9) Zanetti, M.; Kashiwagi, T.; Falqui, L.; Camino, G. *Chem. Mater.* **2002**, *14*, 881−887.
(10) Gilman, J. W.; Harris, R. H.; Shields, J. R.; Kashiwagi, T.; Morgan, A. B. *Polym. Adv. Technol.* **2006**, *17*, 263−271.
(11) Jacquelot, E.; Espuche, E.; Gerard, J. F.; Duchet, J.; Mazabraud, P. *J. Polym. Sci., Part B: Polym. Phys.* **2006**, *44*, 431−440.
(12) Yeh, J. M.; Huang, H. Y.; Chen, C. L.; Su, W. F.; Yu, Y. H. *Surf. Coat. Technol.* **2006**, *200*, 2753−2763.
(13) Yasmin, A.; Abot, J. L.; Daniel, I. M. *Scr. Mater.* **2003**, *49*, 81−86.
(14) Gao, F. *Mater. Today* **2004**, *7*, 50−55.
(15) Arroyo, M.; López-Manchado, M. A.; Herrero, B. *Polymer* **2003**, *44*, 2447−2453.
(16) Zeng, C.; Lee, L. J. *Macromolecules* **2001**, *34*, 4098−4103.
(17) Ren, C.; Du, X.; Ma, L.; Wang, Y.; Zheng, J.; Tang, T. *Polymer* **2010**, *51*, 3416−3424.
(18) Dennis, H. R.; Hunter, D. L.; Chang, D.; Kim, S.; White, J. L.; Cho, J. W.; Paul, D. R. *Polymer* **2001**, *42*, 9513−9522.
(19) Herrera-Alonso, J. M.; Sedlakova, Z.; Marand, E. *J. Membr. Sci.* **2010**, *349*, 251−257.
(20) Ke, Z.; Yongping, B. *Mater. Lett.* **2005**, *59*, 3348−3351.
(21) Picard, E.; Gauthier, H.; Gerard, J. F.; Espuche, E. *J. Colloid Interface Sci.* **2007**, *307*, 364−376.
(22) Medellin-Rodriguez, F. J.; Burger, C.; Hsiao, B. S.; Chu, B.; Vaia, R.; Phillips, S. *Polymer* **2001**, *42*, 9015−9023.
(23) Wang, K.; Liang, S.; Du, R.; Zhang, Q.; Fu, Q. *Polymer* **2004**, *45*, 7953−7960.
(24) Priolo, M. A.; Gamboa, D.; Grunlan, J. C. *ACS Appl. Mater. Interfaces* **2010**, *2*, 312−320.
(25) Ariga, K.; Ji, Q. M.; Hill, J. P.; Bando, Y.; Aono, M. *NPG Asia Mater.* **2012**, *4*, e17-1−e17-11.
(26) *Multilayer Thin Films: Sequential Assembly of Nanocomposite Materials*, 2nd ed.; Decher, G., Schlenoff, J. B., Eds.; Wiley-VCH: Weinheim, Germany, 2012.
(27) Boudou, T.; Crouzier, T.; Ren, K.; Blin, G.; Picart, C. *Adv. Mater.* **2010**, *22*, 441−467.
(28) Priolo, M. A.; Gamboa, D.; Holder, K. M.; Grunlan, J. C. *Nano Lett.* **2010**, *10*, 4970−4974.
(29) Laufer, G.; Priolo, M. A.; Kirkland, C.; Grunlan, J. C. *Green Mater.* **2013**, *1*, 4−10.
(30) Svagan, A. J.; Åkesson, A.; Cárdenas, M.; Bulut, S.; Knudsen, J. C.; Risbo, J.; Plackett, D. *Biomacromolecules* **2012**, *13*, 397−405.
(31) Gu, C.-H.; Wang, J.-J.; Yu, Y.; Sun, H.; Shuai, N.; Wei, B. *Carbohydr. Polym.* **2013**, *92*, 1579−1585.
(32) Findenig, G.; Leimgruber, S.; Kargl, R.; Spirk, S.; Stana-Kleinschek, K.; Ribitsch, V. *ACS Appl. Mater. Interfaces* **2012**, *4*, 3199−3206.
(33) Apaydin, K.; Laachachi, A.; Ball, V.; Jimenez, M.; Bourbigot, S.; Toniazzo, V.; Ruch, D. *Polym. Degrad. Stab.* **2013**, *98*, 627−634.
(34) Li, Y.-C.; Mannen, S.; Morgan, A. B.; Chang, S.; Yang, Y.-H.; Condon, B.; Grunlan, J. C. *Adv. Mater.* **2011**, *23*, 3926−3931.
(35) Laufer, G.; Kirkland, C.; Morgan, A. B.; Grunlan, J. C. *ACS Macro Lett.* **2013**, *2*, 361−365.
(36) Zhai, L.; Cebeci, F. C.; Cohen, R. E.; Rubner, M. F. *Nano Lett.* **2004**, *4*, 1349−1353.
(37) Broderick, A. H.; Manna, U.; Lynn, D. M. *Chem. Mater.* **2012**, *24*, 1786−1795.
(38) Li, Y.; Liu, F.; Sun, J. *Chem. Commun.* **2009**, 2730−2732.
(39) Hammond, P. T. *Mater. Today* **2012**, *15*, 196−206.
(40) Morton, S. W.; Poon, Z.; Hammond, P. T. *Biomaterials* **2013**, *34*, 5328−5335.
(41) De Cock, L. J.; De Koker, S.; De Geest, B. G.; Grooten, J.; Vervaet, C.; Remon, J. P.; Sukhorukov, G. B.; Antipina, M. N. *Angew. Chem., Int. Ed.* **2010**, *49*, 6954−6973.
(42) Chevallier, P.; Turgeon, S.; Sarra-Bournet, C.; Turcotte, R.; Laroche, G. *ACS Appl. Mater. Interfaces* **2011**, *3*, 750−758.
(43) Lee, H.; Alcaraz, M. L.; Rubner, M. F.; Cohen, R. E. *ACS Nano* **2013**, *7*, 2172−2185.
(44) Leterrier, Y. *Prog. Mater Sci.* **2003**, *48*, 1−55.
(45) Affinito, J. D.; Gross, M. E.; Coronado, C. A.; Graff, G. L.; Greenwell, I. N.; Martin, P. M. *Thin Solid Films* **1996**, *290−291*, 63−67.
(46) Yang, Y.-H.; Bolling, L.; Priolo, M. A.; Grunlan, J. C. *Adv. Mater.* **2013**, *25*, 503−508.
(47) Priolo, M. A.; Holder, K. M.; Gamboa, D.; Grunlan, J. C. *Langmuir* **2011**, *27*, 12106−12114.
(48) Cussler, E. L.; Hughes, S. E.; Ward, W. J.; Aris, R. *J. Membr. Sci.* **1988**, *38*, 161−174.
(49) Decher, G. *Science* **1997**, *277*, 1232−1237.
(50) Dubas, S. T.; Schlenoff, J. B. *Macromolecules* **1999**, *32*, 8153−8160.
(51) Advincula, R.; Aust, E.; Meyer, W.; Knoll, W. *Langmuir* **1996**, *12*, 3536−3540.
(52) Lvov, Y.; Ariga, K.; Onda, M.; Ichinose, I.; Kunitake, T. *Colloids Surf., A* **1999**, *146*, 337−346.
(53) Zacharia, N. S.; Modestino, M.; Hammond, P. T. *Macromolecules* **2007**, *40*, 9523−9528.
(54) Bertrand, P.; Jonas, A.; Laschewsky, A.; Legras, R. *Macromol. Rapid Commun.* **2000**, *21*, 319−348.

(55) Sukhorukov, G. B.; Schmitt, J.; Decher, G. *Ber. Bunsenges. Phys. Chem.* **1996**, *100*, 948−953.
(56) von Klitzing, R. *Phys. Chem. Chem. Phys.* **2006**, *8*, 5012−5033.
(57) Kurth, D. G.; Osterhout, R. *Langmuir* **1999**, *15*, 4842−4846.
(58) Ariga, K.; Lvov, Y.; Kunitake, T. *J. Am. Chem. Soc.* **1997**, *119*, 2224−2231.
(59) Schlenoff, J. B.; Dubas, S. T. *Macromolecules* **2001**, *34*, 592−598.
(60) Cho, C.; Valverde, L.; Ozin, G. A.; Zacharia, N. S. *Langmuir* **2010**, *26*, 13637−13643.
(61) Almodovar, J.; Place, L. W.; Gogolski, J.; Erickson, K.; Kipper, M. J. *Biomacromolecules* **2011**, *12*, 2755−2765.
(62) Kunz, D. A.; Schmid, J.; Feicht, P.; Erath, J.; Fery, A.; Breu, J. *ACS Nano* **2013**, *7*, 4275−4280.
(63) Duncan, T. V. *J. Colloid Interface Sci.* **2011**, *363*, 1−24.
(64) Gamboa, D.; Priolo, M. A.; Ham, A.; Grunlan, J. C. *Rev. Sci. Instrum.* **2010**, *81*, 036103-1−036103-3.
(65) Jang, W. S.; Grunlan, J. C. *Rev. Sci. Instrum.* **2005**, 76.
(66) Yang, Y. H.; Haile, M.; Park, Y. T.; Malek, F. A.; Grunlan, J. C. *Macromolecules* **2011**, *44*, 1450−1459.
(67) Priolo, M. A.; Holder, K. M.; Greenlee, S. M.; Stevens, B. E.; Grunlan, J. C. *Chem. Mater.* **2013**, *25*, 1649−1655.
(68) Yang, Y. H.; Malek, F. A.; Grunlan, J. C. *Ind. Eng. Chem. Res.* **2010**, *49*, 8501−8509.
(69) Motschmann, H.; Stamm, M.; Toprakcioglu, C. *Macromolecules* **1991**, *24*, 3681−3688.
(70) Nguyen, C. A.; Argun, A. A.; Hammond, P. T.; Lu, X.; Lee, P. S. *Chem. Mater.* **2011**, *23*, 2142−2149.
(71) Peng, C.; Thio, Y. S.; Gerhardt, R. A. *Langmuir* **2011**, *28*, 84−91.
(72) Lee, S.-W.; Lee, D. *Macromolecules* **2013**, *46*, 2793−2799.
(73) Vidyasagar, A.; Sung, C.; Losensky, K.; Lutkenhaus, J. L. *Macromolecules* **2012**, *45*, 9169−9176.
(74) Jomaa, H. W.; Schlenoff, J. B. *Langmuir* **2005**, *21*, 8081−8084.
(75) Lavalle, P.; Vivet, V.; Jessel, N.; Decher, G.; Voegel, J. C.; Mesini, P. J.; Schaaf, P. *Macromolecules* **2004**, *37*, 1159−1162.
(76) Hoogeveen, N. G.; Stuart, M. A. C.; Fleer, G. J.; Bohmer, M. R. *Langmuir* **1996**, *12*, 3675−3681.
(77) Izumrudov, V.; Kharlampieva, E.; Sukhishvili, S. A. *Macromolecules* **2004**, *37*, 8400−8406.
(78) Sui, Z. J.; Salloum, D.; Schlenoff, J. B. *Langmuir* **2003**, *19*, 2491−2495.
(79) McAloney, R. A.; Goh, M. C. *J. Phys. Chem. B* **1999**, *103*, 10729−10732.
(80) Schoeler, B.; Kumaraswamy, G.; Caruso, F. *Macromolecules* **2002**, *35*, 889−897.
(81) Dubas, S. T.; Schlenoff, J. B. *Macromolecules* **2001**, *34*, 3736−3740.
(82) Picart, C.; Lavalle, P.; Hubert, P.; Cuisinier, F. J. G.; Decher, G.; Schaaf, P.; Voegel, J. C. *Langmuir* **2001**, *17*, 7414−7424.
(83) Podsiadlo, P.; Michel, M.; Lee, J.; Verploegen, E.; Kam, N. W. S.; Ball, V.; Lee, J.; Qi, Y.; Hart, A. J.; Hammond, P. T.; Kotov, N. A. *Nano Lett.* **2008**, *8*, 1762−1770.